Review of Scientific Instruments

Active control of electron cyclotron emission radiometer channel frequencies for improved electron temperature measurements

Cite as: Rev. Sci. Instrum. **92**, 033530 (2021); https://doi.org/10.1063/5.0043662
Submitted: 10 January 2021 . Accepted: 26 February 2021 . Published Online: 12 March 2021

R. Xie, S. Houshmandyar, and M. E. Austin

Active control of electron cyclotron emission radiometer channel frequencies for improved electron temperature measurements

Cite as: Rev. Sci. Instrum. 92, 033530 (2021); doi: 10.1063/5.0043662
Submitted: 10 January 2021 • Accepted: 26 February 2021 •
Published Online: 12 March 2021

R. Xie,[a] S. Houshmandyar, and M. E. Austin

AFFILIATIONS

Institute for Fusion Studies, The University of Texas at Austin, Austin, Texas 78712, USA

Note: Paper published as part of the Special Topic on Proceedings of the 23rd Topical Conference on High-Temperature Plasma Diagnostics.
[a]**Author to whom correspondence should be addressed:** rfxie@utexas.edu

ABSTRACT

As advanced scenarios are developed for tokamak operations, the demand for flexibility of the electron cyclotron emission (ECE) channels' locations has increased. The tunable feature of yttrium iron garnet (YIG) filters provides this spatial flexibility. Here, we present a method of performing ECE measurements on fixed flux surfaces instead of fixed frequencies. This is achieved by adjusting YIG filters utilized in the intermediate frequency section to frequencies associated with flux surfaces in regions of interest during the discharge. The key components are the application of tunable YIG filters and a control program that calculates the filter settings using flux information from real-time reconstruction equilibria (EFIT). This fast procedure facilitates T_e measurements in regions of interest to investigate plasma dynamic behaviors.

I. INTRODUCTION

Electron cyclotron emission (ECE) in magnetically confined plasmas is commonly used to provide measurement of electron temperature with excellent spatial and temporal resolution. Traditional ECE radiometers employ fixed frequency filters in their intermediate frequency (IF) sections. The locations of these fixed frequency channels in terms of flux coordinates often change during a discharge due to a shift in flux surfaces. The change in magnetic fields is another common cause of the ECE location shift. A drift in magnetic field strength will transpose the radial position associated with a certain frequency, which will move the locations of fixed frequency channels. Since both magnetic field strength and flux surfaces are subject to change during a discharge, it is difficult for fixed frequency ECE channels to provide measurements on fixed flux surfaces in regions of interest.

Recently, yttrium iron garnet (YIG) bandpass filters were utilized in the IF sections of ECE diagnostics to implement variable location channels.[1–3] This approach is less complicated than adding a tunable frequency local oscillator (LO) to the existing ECE system, which would require greater modification in a single-sided mixer configuration. These variable location channels are used for turbulent transport studies[1,2] as well as real-time ∇T_e measurements[3] due to the YIG filters' improved sensitivity for T_e fluctuation[4] and temporal resolution.[3]

Moreover, the center frequency of each YIG filters can be individually adjusted, thus repositioning the channel. The center frequency settings are usually tabulated using the magnetic field setting and applied before each discharge. It is noteworthy that this flexibility enables the rearrangement of ECE channels even during a discharge.[3] As a result, it is possible for ECE channels to maintain their views on a fixed region by tuning the YIG filters in real time, so the frequency matches the moving ECE resonance location throughout the discharge duration. In the plasma diagnostics context, this capability can be used to, for example, accurately measure T_e profiles at the pedestal regions of H-mode plasmas by repositioning the ECE channels to radii with high optical thickness ($\tau > 3$). It can also be used in tokamak operation control to provide information to the plasma actuators (e.g., electron cyclotron current drive) to suppress neoclassical tearing modes (NTMs) by collecting T_e and ∇T_e information on a specific rational q surface.[5,6]

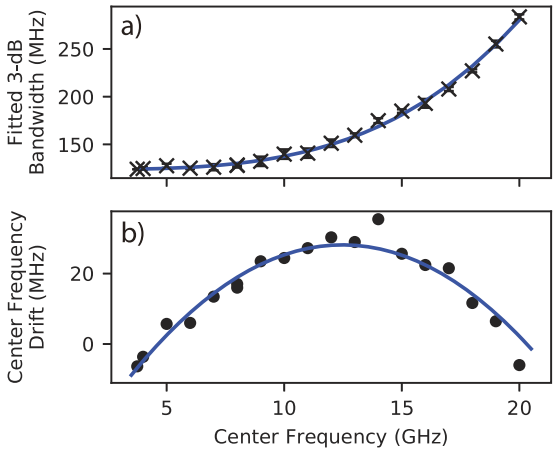

FIG. 1. Frequency dependence of 3-dB bandwidth (a) and center frequency drift (b) for YIG filter 39769. The blue lines represent the least squares power (a) and polynomial (b) fitting.

In this paper, we present a method of performing ECE measurements on fixed flux surfaces instead of fixed frequency using tunable YIG bandpass filters. An experimental result demonstrating the flexibility of YIG bandpass filters is presented in Sec. II. The control scheme and simulation results are shown in Sec. III, and its current limitations are discussed in Sec. IV.

II. FLEXIBILITY OF YIG BANDPASS FILTERS

The control program presented in this paper is designed for the fast modulating/mobile electron cyclotron emission (FMECE) diagnostics system, which uses eight Micro Lambda (MLFP-1710PD) tunable (3.75–20 GHz) and self-shielding bandpass YIG filters with 3-dB bandwidth between 100 and 290 MHz. Each YIG filter's center (set) frequency is adjusted via a 12-bit digital word that is supplied by an NI (PXI-7853R) field programmable gate array (FPGA) controller. The YIG outputs are rectified with Schottky diodes, whose voltage outputs are subsequently amplified and digitized by using the aforementioned FPGA controller. The digitized voltage output will be referred to as the YIG signals for the rest of the discussion.

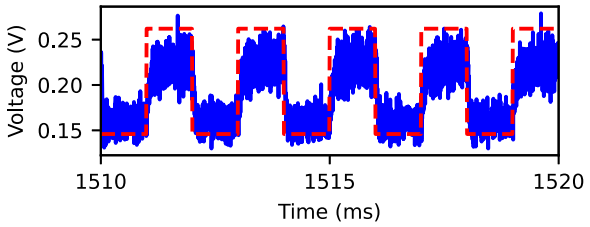

FIG. 2. Output voltage (solid line) for one YIG filter when slewed between two center frequencies during DIII-D discharge 183762. The red dashed line represents the scaled time trace of center frequency setting (low setting: 6 GHz, high setting: 6.1 GHz) for this filter.

The spatial resolution of each YIG filter was bench tested and calibrated using the technique described in Ref. 3. Figure 1 summarizes the calibration result for one of the eight YIG filters and shows the dependence of its 3-dB bandwidth and center frequency drift on the set center frequency. Here, the frequency drift is defined as $\Delta F = F_{fitted} - F_{set}$. The 3-dB bandwidth and frequency drift are fitted with power function $w = aF_{set}{}^{b} + c$ and polynomial function $\Delta F = \alpha F_{set}{}^{2} + \beta F_{set} + \gamma$, respectively. The results for the least squares fittings are summarized in Table I.

In addition, the YIG filters' flexibility has been validated using the ECE signal split from the 81 GHz LO of DIII-D's high resolution fixed frequency channel ECE diagnostic (HRECE).[7] During this validation study, the FMECE is located outside the shield wall, about 20 m away from the DIII-D tokamak, inside the ECE instrument room to minimize the effect of the external magnetic field. Figure 2 compares the voltage output for one FMECE channel and the time trace of its center frequency setting during a DIII-D discharge. The filter was slewed at 1 ms intervals between 6 and 6.1 GHz to measure the real-time electron temperature gradient; mixed with the LO with 81 GHz frequency, the filter was slewed between 87.0 and 87.1 GHz of the second ECE harmonic. It is noteworthy that the voltage signal in Fig. 2 does not display the ringing effect[3] observed in previous generation of YIG filters. This reduces the setting time to less than 1 ms and allows for slew rate up to 1 kHz. Therefore, the coincidence of voltage and center frequency setting steps demonstrates that the YIG filters can be slew during a discharge and provide the flexibility to quickly rearrange ECE channels.

TABLE I. The least squares fit results.

	Serial number (FMECE channel number)							
Parameter	39769 (Ch1)	39770 (Ch4)	39771 (Ch2)	39772 (Ch3)	39980 (Ch7)	39981 (Ch6)	39982 (Ch5)	39983 (Ch8)
a[a]	6.270×10^{-3}	6.263×10^{-3}	8.293×10^{-3}	9.764×10^{-3}	1.666×10^{-2}	1.814×10^{-3}	6.778×10^{-3}	3.774×10^{-3}
b[a]	3.379	3.338	3.253	3.220	2.942	3.768	3.275	3.461
c[a]	123.2	124.1	124.3	129.0	125.7	123.4	119.9	124.8
α[b]	−0.4584	−0.4926	−0.4307	−0.4366	−0.3567	−0.4407	−0.4270	−0.4084
β[b]	11.44	12.88	11.05	11.33	9.22	11.30	10.97	10.55
γ[b]	−43.25	−56.52	−39.76	−46.12	−38.43	−43.36	−42.92	−49.13

[a] 3-dB bandwidth $w = aF_{set}{}^{b} + c$.
[b] Center frequency drift $\Delta F = \alpha F_{set}{}^{2} + \beta F_{set} + \gamma$.

III. CONTROL SCHEME AND SIMULATION RESULTS

A new real-time control system was designed for the FMECE diagnostics currently located at DIII-D. In this approach, the control computer continuously calculates the optimal settings for the FMECE channels using the latest equilibrium. The system consists of the local server storage, control computer, and FPGA controller, and the architect of this control scheme is shown in Fig. 3. The operation of this system is discussed in this section.

A. Control scheme

First, the control computer retrieves flux information from the real-time equilibrium reconstructed using the EFIT code. A dedicated Python code then uses the obtained information to create contours with constant normalized toroidal flux. The code subsequently calculates where the ECE sight line intercepts the flux contours in a region of interest and determines the ECE frequencies at these locations using the local magnetic field strength. Afterward, these settings are transmitted to the FPGA controller, which adjusts the YIG bandpass filters by sending a new 12-bit digital word. This process is repeated until the plasma discharge is complete. In the meanwhile, the FPGA controller continuously digitizes and records the diode voltage outputs. The transmission and digitization processes operate independently of each other and can be executed at the same time utilizing the FPGA controller.

B. Simulation result

The main objective is to keep the FMECE channels aligned with certain flux surfaces to cover a region in flux coordinates throughout the plasma discharge. Figure 4 demonstrates one example of the previously mentioned shift in fixed frequency channels' locations as the DIII-D plasma discharge 171651 transitions from L-mode to H-mode. In this case, this shift led to gaps, ρ (normalized flux coordinate) between 0.9 and 0.95, for example, in the coverage provided by the fixed frequency channels. As indicated in Fig. 5, the shift shown in Fig. 4 is mainly the result of changes in flux surfaces caused by neutral beam injection after 3000 ms. To calibrate and demonstrate the capability of the real-time control code, a simulation has been carried out using existing real-time equilibrium EFITRT1 for the same discharge 171651 shown in Fig. 4.

In this simulation, the available FMECE channels were set to measure electron temperature on flux surfaces with normalized effective radii ρ of 0.85, 0.86, 0.87, 0.88, 0.89, 0.90, 0.91, and 0.92. These values were chosen to cover the edge region but avoid where the plasma is not often optically thick.

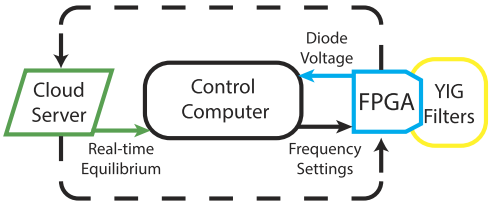

FIG. 3. Diagram of the FMECE real-time control system.

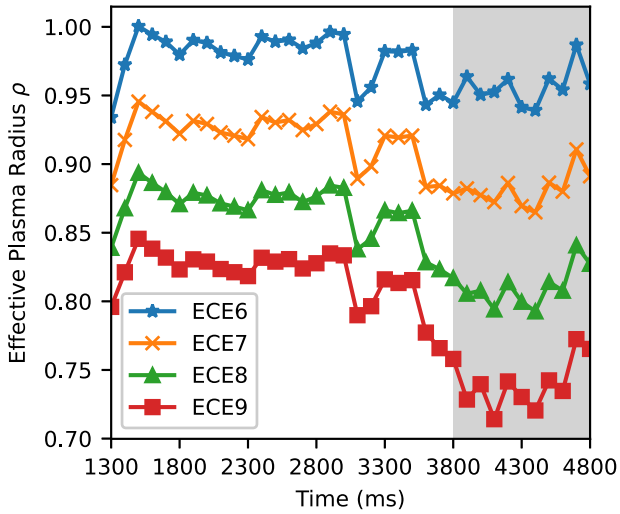

FIG. 4. Locations of four adjacent fixed frequency ECE channels for DIII-D discharge 171651 mapped using EFIT01. This discharge transitioned into H-mode (shaded region) at around 3800 ms.

Figure 6(a) shows the frequency settings for the even-numbered FMECE channels between 1800 ms and 4800 ms. Figure 6(b) plots the locations of the same four channels remapped using EFIT01 for the same period. The color for each trace in this figure is matched with the ones in Fig. 6(a). It is noteworthy that in Fig. 6(b), most of the channels' positions remained within the preset region with ρ between 0.85 and 0.92. Even after the discharge enters into H-mode, the majority of variable location channels still remained inside the region of interest. In Fig. 4, the average location of ECE fixed frequency channel 8 is $\rho \approx 0.877$ between 1400 and 3000 ms. When the

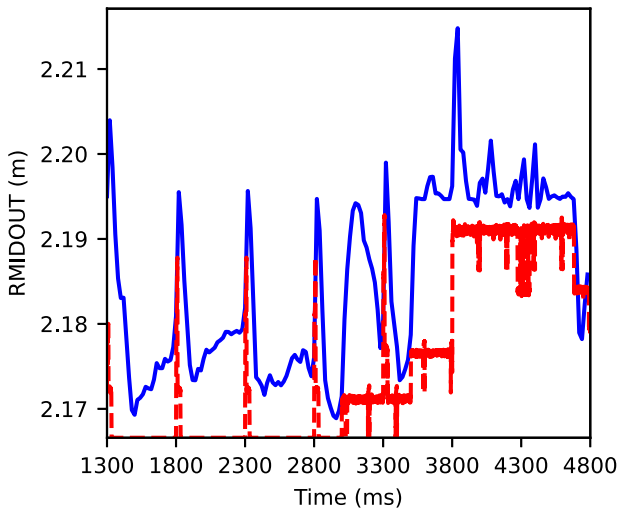

FIG. 5. Time evolution of EFIT point name RMIDOUT (solid line), which stands for the major radius of outer separatrix at the midplane, and scaled neutral beam heating power (dashed line).

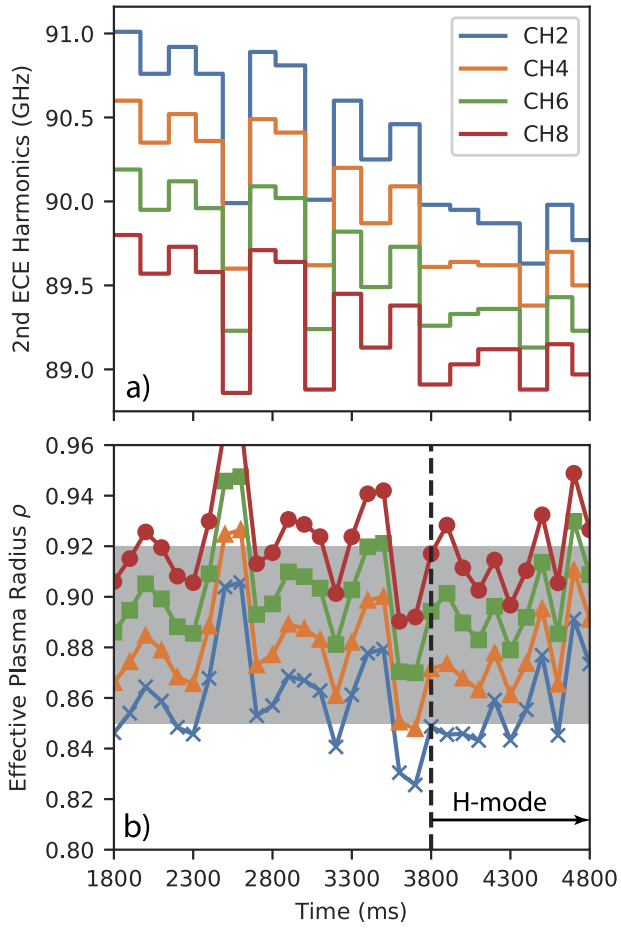

FIG. 6. Frequency settings of the even-numbered channels (a). Locations of the even-numbered variable location channels mapped using EFIT01. The shaded region represents the preset region of interest. The lines from bottom to top stand for channel 2 to channel 8, respectively (b).

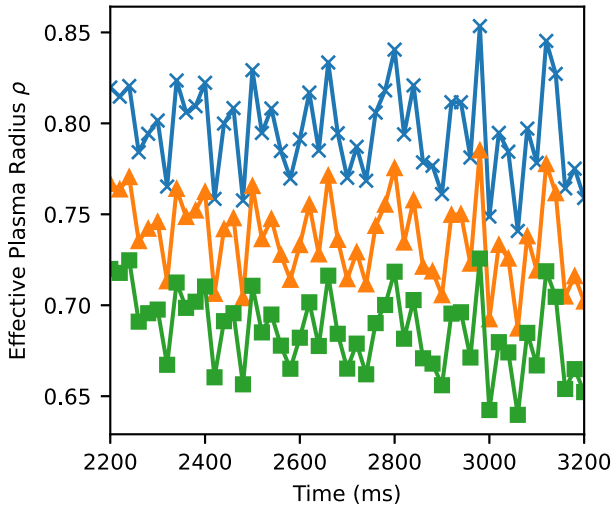

FIG. 7. Locations of three adjacent fixed frequency ECE channels for DIII-D discharge 183780 mapped using EFIT01. The traces from top to bottom represent ECE fixed frequency channels 3, 4, and 5.

plasma is in H-mode between 3800 and 4700 ms, this channel's average location shifted by ~8% to $\rho \approx 0.809$. In comparison, the average location of variable location channel 4 (set to $\rho = 0.88$) shown in Fig. 6(b) shifted from $\rho \approx 0.888$ (between 1400 and 3000 ms) by less than 1.5% to $\rho \approx 0.876$ (between 3800 and 4700 ms). This demonstrates that the real-time control program is capable of responding to changes in plasma conditions and relocating the variable location channels to provide continuous coverage.

IV. CONSTRAINTS AND LIMITATIONS

For the simulation presented in Sec. III, the average time between each frequency adjustment is below 200 ms. The most time consuming process is retrieving equilibrium from the local server, which takes ~150 ms but can take up to 1 s depending on the server load. If this occurs during a discharge, it will limit the temporal flexibility of YIG channels. Since plasma conditions are unlikely to stay relatively constant during this extended period of time, this bottleneck will consequently lead to the deterioration of FMECE coverage. In order to provide an accurate coverage, the FMECE channels should be updated as frequently as the real-time equilibrium. It is noteworthy that the real-time equilibrium is typically calculated every 20 ms at DIII-D, which is significantly faster than the current control program.

In addition, the flux surface corresponding to a certain frequency can change rapidly between each frequency modulation, which will also shift the coverage provided by FMECE channels. Figure 7 shows the time evolution of locations for three fixed frequency ECE channels during a recent DIII-D discharge. Note that in the figure, the channel locations can oscillate by as much as 0.1 effective radius in a given 200 ms window. Due to the limited temporal resolution, it will be challenging for the current real-time control program to capture this type of oscillation.

V. CONCLUSION AND FUTURE WORK

Utilizing the spatial flexibility of the YIG bandpass filters, a new real-time control scheme that allows for ECE measurements on fixed flux surfaces has been demonstrated through simulation. This capability will allow for high resolution T_e measurements in specific regions and help providing insights into plasma dynamics in advanced tokamak scenarios. In addition, the simulation result shows promise in demonstrating that variable location channels can be employed, even in existing IF sections, to design innovative plasma diagnostics.

Future work includes the enhancement of program operation speed to further reduce the time between each frequency modulation. In addition, an algorithm that can provide locations of $q = m/n$ rational surfaces will be integrated into the control program. This will allow the ECE diagnostics to detect island formation and generate information that can be used by actuators to suppress NTMs.

ACKNOWLEDGMENTS

This work was supported by the U.S. Department of Energy OFES under Award Nos. DE-FG02-97ER54415, DE-FC02-04ER54698, and DE-SC0010500.

This report was prepared as an account of work sponsored by an agency of the United States Government. Neither the United States Government nor any agency thereof, nor any of their employees, makes any warranty, express or implied, or assumes any legal liability or responsibility for the accuracy, completeness, or usefulness of any information, apparatus, product, or process disclosed, or represents that its use would not infringe privately owned rights. Reference herein to any specific commercial product, process, or service by trade name, trademark, manufacturer, or otherwise does not necessarily constitute or imply its endorsement, recommendation, or favoring by the United States Government or any agency thereof. The views and opinions of authors expressed herein do not necessarily state or reflect those of the United States Government or any agency thereof.

DATA AVAILABILITY

The data that support the findings of this study are available from the corresponding author upon reasonable request.

REFERENCES

[1]H. Zhao, T. Zhou, Y. Liu, A. Ti, B. Ling, X. Feng, A. D. Liu, C. Zhou, and L. Hu, Fusion Eng. Des. **149**, 111336 (2019).
[2]M. Fontana, L. Porte, and P. Molina Cabrera, Rev. Sci. Instrum. **88**, 083506 (2017).
[3]S. Houshmandyar, M. E. Austin, M. W. Brookman, Y. Liu, W. L. Rowan, and H. Zhao, Rev. Sci. Instrum. **89**, 10H109 (2018).
[4]M. Fontana, L. Porte, S. Coda, O. Sauter, and TCV Team, Nucl. Fusion **58**, 024002 (2017).
[5]E. Kolemen, A. S. Welander, R. J. La Haye, N. W. Eidietis, D. A. Humphreys, J. Lohr, V. Noraky, B. G. Penaflor, R. Prater, and F. Turco, Nucl. Fusion **54**, 073020 (2014).
[6]S. Houshmandyar, R. Xie, M. E. Austin, W. L. Rowan, and H. Zhao, Rev. Sci. Instrum. **92**, 033510 (2021).
[7]D. D. Truong and M. E. Austin, Rev. Sci. Instrum. **85**, 11D814 (2014).